

Scaling of the elastic proton-proton cross-section*

MICHAŁ PRASZAŁOWICZ⁽¹⁾, CRISTIAN BALDENEGRO⁽¹⁾,
CHRISTOPHE ROYON⁽³⁾, ANNA M. STAŚTO⁽⁴⁾

⁽¹⁾Institute of Theoretical Physics, Jagiellonian University,
S. Łojasiewicza 11, 30-348 Kraków, Poland,

⁽²⁾Dipartimento di Fisica, Sapienza Università di Roma,
Piazzale Aldo Moro, 2, 00185 Rome, Italy,

⁽³⁾Department of Physics and Astronomy,
The University of Kansas, Lawrence, KS 66045, USA,

⁽⁴⁾Department of Physics, Penn State University,
University Park, PA 16802, USA.

Received January 16, 2025

We discuss scaling properties of the elastic pp cross-section both at the ISR and the LHC. We observe that the ratio of bump to dip positions of the differential cross-section $d\sigma_{el}/dt$ is constant over the wide energy range. We next study the consequences of this property, including geometric scaling at the ISR and a new scaling laws at the LHC.

1. Introduction

In this note we recapitulate results on the scaling laws of the pp cross-sections (elastic, inelastic and total) discussed in Refs. [1, 2] and [3, 4] (see also [5, 6]). We use data at two energy ranges: ISR [7, 8] covering $W = \sqrt{s} \simeq 20 \div 60$ GeV and LHC TOTEM [9]–[14] of $W \simeq 3 \div 13$ TeV (the ATLAS measurements have focused only on the low $|t|$ region [15, 16]).

Energy behavior of integrated pp cross-sections at both energy ranges is very different. At the ISR, elastic, inelastic and total cross-sections have almost the same energy dependence [8]. This observation led to the concept of geometric scaling [17, 18]. This is not true at the LHC [11]. In Ref. [1] we parametrized pp , cross-sections by the power laws shown in Table 1.

Differential elastic pp cross-sections also reveal significant differences, even though the general *dip-bump* structure is similar. The bump-to-dip

* Presented at “Diffraction and Low- x 2024”, Trabia (Palermo, Italy), September 8-14, 2024.

| | elastic | inelastic | total | $\frac{\text{elastic}}{\text{inelastic}}$ |
|-----|-------------------------|-------------------------|-------------------------|---|
| ISR | $W^{0.1142 \pm 0.0034}$ | $W^{0.1099 \pm 0.0012}$ | $W^{0.1098 \pm 0.0012}$ | $W^{0.0043 \pm 0.0036}$ |
| LHC | $W^{0.2279 \pm 0.0228}$ | $W^{0.1465 \pm 0.0133}$ | $W^{0.1729 \pm 0.0163}$ | $W^{0.0814 \pm 0.0264}$ |

Table 1. Energy dependence of the integrated cross-sections for the energies $W = \sqrt{s}$ at the ISR [8] and at the LHC [19].

cross-section ratio

$$\mathcal{R}_{\text{bd}}(s) = \frac{d\sigma_{\text{el}}/d|t|_{\text{b}}}{d\sigma_{\text{el}}/d|t|_{\text{d}}} \quad (1)$$

saturates at the LHC at approximately 1.8, and is rather strongly energy dependent at the ISR (see e.g. Fig. 2 in Ref. [14]).

However, even for differential cross-sections, there are some regularities that are common both to the ISR and the LHC. First, the smallness of the real part of the forward elastic amplitude encoded in the so called ρ parameter. Second, in Ref. [1] we explored another regularity, namely the ratio of bump-to-dip *positions* in $|t|$ at a given energy

$$\mathcal{T}_{\text{bd}}(s) = |t_{\text{b}}|/|t_{\text{d}}|, \quad (2)$$

which is constant at all energies from the ISR to the LHC and equal to 1.355 ± 0.011 [1], see Table 2. This suggests a scaling variable

$$\tau = f(s)|t| \quad (3)$$

where $f(s)$ is a universal function of energy. Elastic differential cross-sections at different energies, if plotted in terms of τ , will have dips and bumps at exactly the same values of $\tau_{\text{d,b}}$.

2. Geometric scaling at the ISR

Unitarity constraints allow to write scattering cross sections in the impact parameter space

$$\begin{aligned} \sigma_{\text{el}} &= \int d^2\mathbf{b} \left| 1 - e^{-\Omega(s,b) + i\chi(s,b)} \right|^2, \\ \sigma_{\text{tot}} &= 2 \int d^2\mathbf{b} \operatorname{Re} \left[1 - e^{-\Omega(s,b) + i\chi(s,b)} \right], \\ \sigma_{\text{inel}} &= \int d^2\mathbf{b} \left[1 - \left| e^{-\Omega(s,b)} \right|^2 \right] \end{aligned} \quad (4)$$

in terms of the opacity $\Omega(s,b)$ and phase $\chi(s,b)$, which is responsible for the nonzero ρ parameter [20, 21]. However, since the ρ parameter is very small, we can neglect $\chi(s,b)$ in the first approximation.

| | W | dip | | bump | | ratios | |
|-----------|-------|---------|------------------|---------|--------------------|-----------|------------------|
| | | $ t _d$ | error | $ t _b$ | error | t_b/t_d | error |
| LHC [TeV] | 13.00 | 0.471 | +0.002 -0.003 | 0.6377 | +0.0006 -0.0006 | 1.355 | +0.008 -0.005 |
| | 8.00 | 0.525 | +0.002 -0.004 | 0.700 | +0.010 -0.008 | 1.335 | +0.021 -0.016 |
| | 7.00 | 0.542 | +0.012 -0.013 | 0.702 | +0.034 -0.034 | 1.296 | +0.069 -0.069 |
| | 2.76 | 0.616 | +0.001 -0.002 | 0.800 | +0.127 -0.127 | 1.298 | +0.206 -0.206 |
| ISR [GeV] | 62.50 | 1.350 | +0.011 -0.011 | 1.826 | +0.016 -0.039 | 1.353 | +0.016 -0.029 |
| | 52.81 | 1.369 | +0.006 -0.006 | 1.851 | +0.014 -0.018 | 1.352 | +0.012 -0.014 |
| | 44.64 | 1.388 | +0.003 -0.007 | 1.871 | +0.031 -0.015 | 1.348 | +0.023 -0.011 |
| | 30.54 | 1.434 | +0.001 -0.004 | 1.957 | +0.013 -0.028 | 1.365 | +0.010 -0.020 |
| | 23.46 | 1.450 | +0.005 -0.004 | 1.973 | +0.011 -0.018 | 1.361 | +0.009 -0.013 |

Table 2. Positions of bumps obtained by fitting a parabola, and position of dips obtained by fitting a parabola (LHC) or a third order polynomial (ISR), Ref. [1].

Geometric scaling (GS) is a hypothesis [17] that

$$\Omega(s, b) = \Omega(b/R(s)) , \quad (5)$$

where $R(s)$ is the interaction radius [17] increasing with energy. Changing the integration variable in (4) $\mathbf{b} \rightarrow \mathbf{B} = \mathbf{b}/R(s)$ leads to

$$\int d^b \mathbf{b} \dots = R^2(s) \int d^2 \mathbf{B} \dots . \quad (6)$$

Here the integral over $d^2 \mathbf{B}$ is an energy-independent constant. Therefore, the integrated pp cross-sections should scale with energy in the same way. As seen from Table 1, this is indeed the case.

Ref. [18] analyzed the consequences of GS for the differential rather than integrated pp elastic cross-section assuming the following scaling variable

$$\tau = \sigma_{\text{inel}}(s) |t| = R^2(s) |t| \times \text{const}. \quad (7)$$

One can show [18] that in this case function $\Phi(\tau)$ defined as

$$\Phi(\tau) = \frac{1}{\sigma_{\text{inel}}^2(s)} \frac{d\sigma_{\text{el}}}{d|t|}(s, t) \quad (8)$$

should not depend on energy. In Fig. 1 we plot the ISR data before and after scaling. We see that the cross-sections overlap after scaling, except for the dip region. In Ref. [1] we have quantified the quality of this overlap by plotting ratios of the scaled cross-sections in terms of τ .

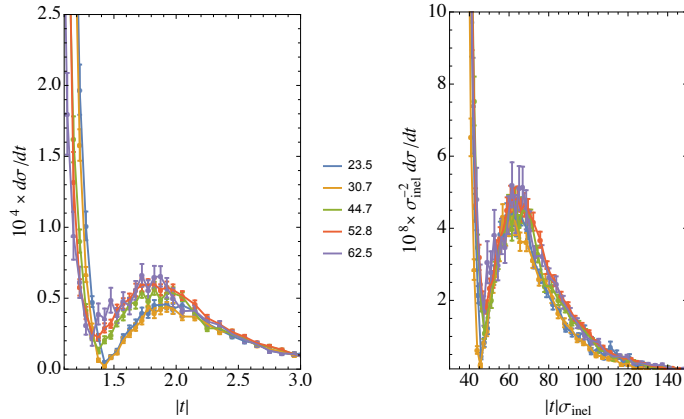


Fig. 1. Elastic pp cross-section $d\sigma_{\text{el}}/dt$ [mb/GeV 2] at the ISR multiplied by 10^4 – left, multiplied by 10^8 and scaled according to Eqs. (8,7) – right.

3. The LHC scaling

As can be seen from Table 1 the energy behavior of the pp cross-sections at the LHC is not universal and therefore GS does not hold, although the scaling variable (3) still superimposes positions of dips and bumps (but not the values of the cross-sections). However, at the LHC ratios \mathcal{R}_{bd} (1) are (almost) energy independent, which suggests a new universal behavior

$$\frac{d\sigma_{\text{el}}}{dt}(t_{\text{d}}) = g(s) \text{const}_{\text{d}}, \quad \frac{d\sigma_{\text{el}}}{dt}(t_{\text{b}}) = g(s) \text{const}_{\text{b}}. \quad (9)$$

Therefore, we expect that dips and bumps at the LHC will overlap when the differential cross-section will be scaled by two functions $f(s)$ and $g(s)$ rather than by one function as was the case at the ISR.¹

Fitting dip and bump positions with a power law, i.e. $f(W) = BW^{-\beta}$ in Eq. (3) one obtains

$$t_{\text{dip}}(W) = (0.732 \pm 0.003) \times (W/(1 \text{ TeV}))^{-0.1686 \pm 0.0027}, \\ t_{\text{bump}}(W) = 1.355 \times t_{\text{dip}}(W). \quad (10)$$

Now, if we plot $d\sigma_{\text{el}}/d|t|$ in terms of the variable $\tau = (W/(1 \text{ TeV}))^{0.1686} |t|$, the dip and bump positions are aligned, as seen in Fig. 2.

Next, we aim at superimposing all curves in the right panel of Fig. 2 shifting them vertically by an energy dependent factor. To this end we try a simple transformation (9)

$$\frac{d\sigma_{\text{el}}}{d|t|}(\tau) \rightarrow \left(\frac{W}{1 \text{ TeV}} \right)^{-\alpha} \frac{d\sigma_{\text{el}}}{d|t|}(\tau). \quad (11)$$

¹ Strictly speaking the cross-section is scaled by g and the scaling variable by f .

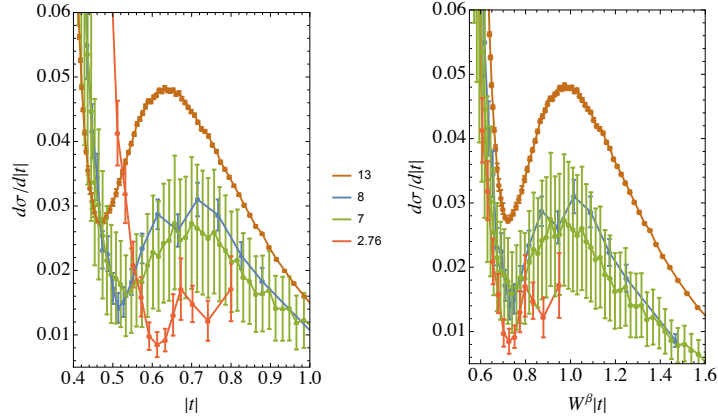


Fig. 2. Elastic pp cross-section $d\sigma_{\text{el}}/dt$ [mb/GeV 2] at the LHC energies in terms of $|t|$ [GeV 2] – left, and in terms of the scaling variable $W^\beta |t|$ – right. We can see that dip and bumps are aligned after scaling.

The results are shown in Fig. 3 for three values of α for fixed $\beta = 0.1686$. In the three panels of Fig. 3 elastic cross-sections overlap or nearly overlap in comparison with the right panel of Fig. 2, indicating scaling. In Ref. [1] we estimated the best value to be $\alpha = 0.66$ with large systematic error. Obviously, global fits may result in different values of α and β .

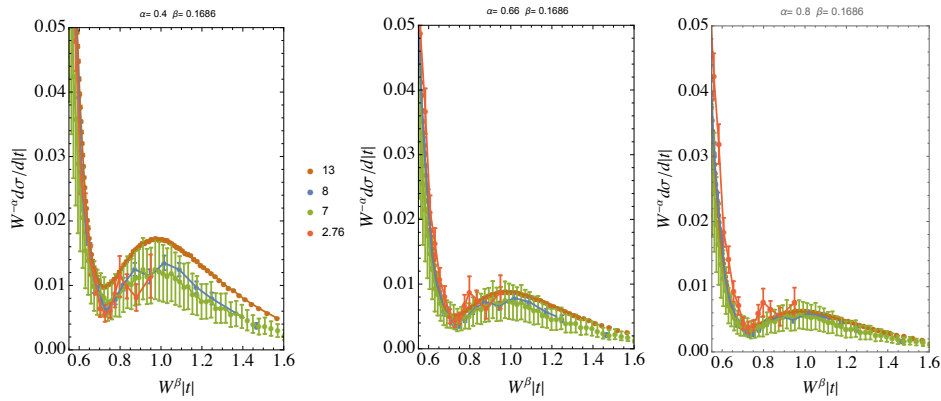


Fig. 3. Scaled elastic pp cross-section $d\sigma_{\text{el}}/dt$ [mb/GeV 2] at the LHC energies in terms of the scaling variable $W^\beta |t|$ for $\beta = 0.1686$ and for $\alpha = 0.4$ (left), $\alpha = 0.66$ (middle) and $\alpha = 0.8$ (right).

4. Other scaling laws

In Ref. [2] another scaling law for the LHC data was proposed. There $\Phi(\tilde{\tau})$ (8) depended on the scaling variable defined as

$$\tilde{\tau} = s^a t^b. \quad (12)$$

Best values of a and b were obtained by minimizing the so called *quality factor* (QF) [22, 23, 24] with the result $\alpha \simeq 0.61$ and $a \simeq 0.065$, $b \simeq 0.72$.

To relate this scaling to the scaling of Sec. 3 let's note that if (12) should align the dips (and bumps) at all LHC energies, the scaled dip (bump) positions

$$\tilde{\tau}_d = s^a t_d^b = s^{a-b\beta/2} B_{\text{dip}}^b \quad (13)$$

should be energy independent. Here we used (3) with $f(s) = B s^{-\beta/2}$. From the energy independence of (13) we obtain

$$a - b\beta/2 = 0. \quad (14)$$

Substituting b from [2] and $\beta = 0.1686$ we find $a = b\beta/2 = 0.061 \pm 0.001$ as compared to $a = 0.065$ from Ref. [2]. Furthermore, our result for the power $\alpha = 0.66$, which is poorly constrained by the data, is again in qualitative agreement with [2], where $\alpha = 0.61$. Obviously Eq. (14) implies the whole family of scaling laws. In a less restricted setup also the parameter β should be determined from global fits.

5. Summary and conclusions

We explored the property that (t_b/t_d) is constant over three orders of magnitude in energy. This behavior suggests a universal behavior of the elastic scattering cross-sections as a function of a scaling variable $\tau = f(s)|t|$.

Such transformation was sufficient at the ISR, but at the LHC one had to modify the values of the cross-sections by another scaling function $g(s)$. This difference may be related to the saturation [2]. For the consequences of the above scaling for the phenomenological parameterizations of the scattering amplitude, see Ref. [1].

Acknowledgments

MP thanks the organizers for a fruitful and stimulating workshop. AMS is supported by the U.S. Department of Energy grant No. DE-SC-0002145 and within the framework of the Saturated Glue (SURGE) Topical Theory Collaboration. CB is supported by the European Research Council consolidator grant no. 101002207.

REFERENCES

- [1] C. Baldenegro, M. Praszalowicz, C. Royon and A. M. Stasto, *Phys. Lett. B* **856** (2024), 138960.
- [2] C. Baldenegro, C. Royon and A. M. Stasto, *Phys. Lett. B* **830** (2022), 137141.
- [3] C. Royon, C. Baldenegro and A. Stasto, *PoS ICHEP2022* (2022), 762.
- [4] M. Praszalowicz, C. Baldenegro, C. Royon and A. M. Stasto, [arXiv:2407.13805 [hep-ph]].
- [5] I. M. Dremin and V. A. Nechitailo, *Phys. Lett. B* **720**, 177-180 (2013).
- [6] T. Csörgő, T. Novak, R. Pasechnik, A. Ster and I. Szanyi, *Eur. Phys. J. C* **81**, no.2, 180 (2021).
- [7] E. Nagy, R. S. Orr, W. Schmidt-Parzefall, K. Winter, A. Brandt, F. W. Busser, G. Flugge, F. Niebergall, P. E. Schumacher and H. Eichinger, *et al. Nucl. Phys. B* **150**, 221-267 (1979).
- [8] U. Amaldi and K. R. Schubert, *Nucl. Phys. B* **166**, 301-320 (1980).
- [9] G. Antchev *et al.* [TOTEM], *EPL* **95**, no.4, 41001 (2011).
- [10] G. Antchev *et al.* [TOTEM], *Nucl. Phys. B* **899**, 527-546 (2015).
- [11] G. Antchev *et al.* [TOTEM], *Eur. Phys. J. C* **79**, no.2, 103 (2019).
- [12] G. Antchev *et al.* [TOTEM], *Eur. Phys. J. C* **79**, no.9, 785 (2019).
- [13] G. Antchev *et al.* [TOTEM], *Eur. Phys. J. C* **80**, no.2, 91 (2020).
- [14] V. M. Abazov *et al.* [TOTEM and D0], *Phys. Rev. Lett.* **127**, no.6, 062003 (2021).
- [15] G. Aad *et al.* [ATLAS] *Nucl. Phys.* **889** 486 (2014).
- [16] G. Aad *et al.* [ATLAS] *EPJC* **83** 5, 441, (2023).
- [17] J. Dias De Deus, *Nucl. Phys. B* **59**, 231-236 (1973)
- [18] A. J. Buras and J. Dias de Deus, *Nucl. Phys. B* **71**, 481-492 (1974).
- [19] F. J. Nemes [TOTEM], *PoS DIS2019*, 065 (2019).
- [20] V. Barone and E. Predazzi, "High-Energy Particle Diffraction," Springer-Verlag Berlin Heidelberg, 2002.
- [21] E. Levin, [arXiv:hep-ph/9808486 [hep-ph]].
- [22] F. Gelis, R. B. Peschanski, G. Soyez and L. Schoeffel, *Phys. Lett. B* **647**, 376-379 (2007).
- [23] G. Beuf, R. Peschanski, C. Royon and D. Salek, *Phys. Rev. D* **78**, 074004 (2008).
- [24] C. Marquet and L. Schoeffel, *Phys. Lett. B* **639**, 471-477 (2006).